

# The pathogenic mechanism of diabetes varies with the degree of overexpression and oligomerization of human amylin in the pancreatic islet $\beta$ cells

Shaoping Zhang,<sup>\*,†</sup> Hong Liu,<sup>\*</sup> Chia Lin Chuang,<sup>\*</sup> Xiaoling Li,<sup>\*</sup> Maggie Au,<sup>\*</sup> Lin Zhang,<sup>\*</sup> Anthony R. J. Phillips,<sup>\*,†</sup> David W. Scott,<sup>\*</sup> and Garth J. S. Cooper<sup>\*,†,‡,§,1</sup>

<sup>\*</sup>The School of Biological Sciences and <sup>†</sup>The Maurice Wilkins Centre for Molecular BioDiscovery, Faculty of Science, University of Auckland, Auckland, New Zealand <sup>‡</sup>Centre for Advanced Discovery and Experimental Therapeutics, Central Manchester University Hospitals National Health Service (NHS) Foundation Trust, Manchester, UK; and <sup>§</sup>Centre for Endocrinology and Diabetes, Institute of Human Development, Faculty of Medical and Human Sciences, Manchester Academic Health Sciences Centre, The University of Manchester, Manchester, UK

**ABSTRACT** The aggregation of human amylin (hA) to form cytotoxic structures has been closely associated with the causation of type 2 diabetes. We sought to advance understanding of how altered expression and aggregation of hA might link  $\beta$ -cell degeneration with diabetes onset and progression, by comparing phenotypes between homozygous and hemizygous hA-transgenic mice. The homozygous mice displayed elevated islet hA that correlated positively with measures of oligomer formation ( $r=0.91$ ;  $P<0.0001$ ). They also developed hyperinsulinemia with transient insulin resistance during the prediabetes stage and then underwent rapid  $\beta$ -cell loss, culminating in severe juvenile-onset diabetes. The prediabetes stage was prolonged in the hemizygous mice, wherein  $\beta$ -cell dysfunction and extensive oligomer formation occurred in adulthood at a much later stage, when hA levels were lower ( $r=-0.60$ ;  $P<0.0001$ ). This is the first report to show that hA-evoked diabetes is associated with age, insulin resistance, progressive islet dysfunction, and  $\beta$ -cell apoptosis, which interact variably to cause the different diabetes syndromes. The various levels of hA elevation cause different extents of oligomer formation in the disease stages, thus eliciting early- or adult-onset diabetes syndromes, reminiscent of type 1 and 2 diabetes, respectively. Thus, the hA-evoked diabetes phenotypes differ substantively according to degree of amylin overproduction. These findings are relevant to the understanding of the pathogenesis and the development of experimental therapeutics for diabetes.—Zhang, S., Liu, H., Chuang, C. L., Li, X., Au, M., Zhang, L., Phillips, A R. J., Scott, D. W., Cooper, G. J. S. The

pathogenic mechanism of diabetes varies with the degree of overexpression and oligomerization of human amylin in the pancreatic islet  $\beta$  cells. *FASEB J.* 28, 000–000 (2014). [www.fasebj.org](http://www.fasebj.org)

*Key Words:* gene-dosage effect • apoptosis • peptide aggregation • transgenic mice • insulin resistance

ONE OF THE MAIN PATHOLOGICAL hallmarks of type 2 diabetes is the presence of islet amyloid deposits composed primarily of human amylin [hA; also called islet amyloid polypeptide (IAPP); refs. 1, 2]. hA is a 37-aa peptide that is normally soluble and is cosecreted with insulin from islet  $\beta$  cells in response to physiological stimuli (3, 4). It exhibits innate physicochemical properties that predispose it to aggregate and form fibrils in physiopathological conditions such as type 2 diabetes (5–7). These processes are linked to the triggering of  $\beta$ -cell apoptosis and are thought to play a role in the causation and progression of  $\beta$ -cell destruction in type 2 diabetes (8–10). In contrast, murine amylin (mA) is nonfibrillogenic and displays no cytotoxicity toward  $\beta$  cells (5, 11–13). Therefore, to study the cytotoxic and diabetogenic properties of hA *in vivo*, it is necessary to generate hA transgenic rodents. The exact processes that lead hA to aggregate in patients with diabetes remain incompletely understood.

There is substantive evidence, from studies in cultured  $\beta$  cells and islets, as well as *in vivo* studies in transgenic mice, that fibrillogenic hA elicits apoptosis *via* activation of several cell-signaling pathways (8, 10, 14–16). Aggregate membrane interactions may be necessary to trigger the apoptotic process (10). Several death-signaling or -inducing molecules, including Fas, FasL, and FADD, have been shown to contribute to  $\beta$ -cell destruction (17). In addition, activation of pathways comprising caspases-8 and -3, JNK1, and p38

Abbreviations: AOLIM, amylin oligomer-like immunoreactive material; BW, body weight; *Gck*, glucokinase; *Glut2*, glucose transporter 2; hA, human amylin; IAPP, islet amyloid polypeptide; IGT, impaired glucose tolerance; *Ins1*, insulin 1; *Ins2*, insulin 2; IPGTT, intraperitoneal glucose tolerance test; IPITT, intraperitoneal insulin tolerance test; mA, murine amylin; qPCR, quantitative polymerase chain reaction; RT-qPCR, reverse transcription-quantitative polymerase chain reaction

<sup>1</sup> Correspondence: School of Biological Sciences, University of Auckland, 3 Symonds Street, Auckland 1010, New Zealand. E-mail: [g.cooper@auckland.ac.nz](mailto:g.cooper@auckland.ac.nz)  
doi: 10.1096/fj.14-251744

kinase (18–21), along with membrane disruption and pore formation (22), increased ER stress, and oxidative stress, have all been implicated in the pathways that lead to or cause hA-evoked  $\beta$ -cell apoptosis (23–26).

Recent studies of the cytotoxicity of hA have provided evidence that soluble oligomers and aggregates formed from hA could be more cytotoxic than mature fibrils (12, 14, 20, 27–29) and may act as novel targets for therapeutic intervention. The aggregation potential of hA determines its cytotoxicity to  $\beta$  cells (27). However, there is also contradictory evidence against the hypothesis of oligomer-mediated toxicity (30, 31). Some have argued that there is insufficient evidence at present to prove conclusively that the oligomers act as the sole or even the most important culprit (16). Therefore, more direct evidence concerning the cytotoxicity of hA in oligomeric form is needed to better understand its role in the mechanism of  $\beta$ -cell death.

Various rodent models transgenic for hA have been developed to enable investigation of the *in vivo* effects of hA overexpression in oligomer aggregation and amyloid fibril formation and its consequent impacts on islet cell function, systemic metabolic regulation, and the pathogenesis of diabetes (15, 24, 28, 32–39). It has been reported that elevated production of hA in mouse and rat islet  $\beta$  cells may not always be sufficient to cause islet degeneration and diabetes and that additional factors may initiate islet amyloid formation and disease onset and progression (15, 32, 34, 35, 37, 40).

We generated a line of hA-transgenic mice in which hemizygous animals develop spontaneous diabetes leading to progressive  $\beta$ -cell loss with very high penetrance ( $\geq 90\%$ ). More severely affected individuals, namely those with early-onset diabetes, do not necessarily have detectable islet amyloid at all during their diabetic syndrome, pointing to the existence of a cytotoxic stimulus other than mature fibrils (38, 39). However, the potential roles of toxic oligomers in  $\beta$ -cell death (loss) and the development of diabetes in these animals have not been investigated.

Here, we report our detailed characterization of this transgenic line by comparison between hemizygous and homozygous transgenic animals. The latter were found to express higher levels of hA and manifest a much earlier onset diabetic syndrome than were the hemizygous individuals. These findings demonstrate a gene–dosage effect in hA-elicited diabetes. We also asked whether there is evidence of formation of hA oligomers in the islets of homozygous or hemizygous transgenic animals without the concomitant presence of microscopic amyloid deposits; whether evidence of hA oligomers manifests within or without  $\beta$  cells; and how evidence of their formation might relate temporally to pancreatic hormone levels,  $\beta$ -cell dysfunction, systemic metabolic regulation, and the onset and progression of diabetes.

## MATERIALS AND METHODS

### Animals

All experiments were approved by the Animal Ethics Committee of the University of Auckland, and the study was

performed according to the Guide for the Care and Use of Laboratory Animals (41).

We used a line of FVB/N mice transgenic for hA cDNA (designated L13) that express the hormone almost exclusively in their islet  $\beta$  cells (38, 39). The transgene is expressed under the control of the rat insulin 2 promoter (38, 39), and different lines created by separate pronuclear injections have similar phenotypes, excluding insertional mutagenesis, as an explanation of the observed diabetes phenotypes. In this study, male animals were used in all experiments to avoid the untoward variability introduced by the estrous cycle in females. They were generated from  $(+/-) \times (+/-)$  crosses and weaned on d 21 after birth, and glucose and body weight (BW) were monitored twice weekly thereafter. All the animals were genotyped by quantitative polymerase chain reaction (qPCR) of tail-tip DNA, to identify homozygous or hemizygous mice, and their respective nontransgenic littermates were used as age-matched controls for all experiments (38).

Diabetes was diagnosed when casual blood glucose levels were  $>11$  mM on 2 consecutive measurements  $\geq 3$  d apart (41). Classic symptoms of diabetes, such as moderate polyuria and polydipsia, begin to appear in these mice when their glucose levels are  $>11$  mM. All genotyped transgenic and nontransgenic littermates were killed at the stated stages of diabetes (prediabetes and early-, mid-, late- or end-stage disease, respectively), as determined by the tail-vein nonfasting blood glucose measurements detailed below.

The stages of diabetes were defined as follows.

### *Prediabetes*

Blood glucose values were significantly higher than those in matched nontransgenic controls but insufficient to support the diagnosis of diabetes ( $\leq 11$  mM). In all experiments, the mice were used only after they were weaned; although prediabetes may be present in homozygous mice during the suckling period, lactation may interfere with interpretation of data and was thus avoided.

### *Early diabetes*

Stage occurred at and soon after disease onset, when blood glucose values were typically in the 11–14 mM range.

### *Mid-diabetes*

Blood glucose values were typically in the 18–22 mM range.

### *Late diabetes*

Blood glucose values reached  $\geq 28$  mM, but terminal signs were absent.

### *End diabetes*

The terminal stage of the disease, when animals maintained blood glucose levels of  $\geq 33$  mM but, in addition, displayed  $\geq 1$  of the following characteristics, thereby meeting pre-defined and approved criteria for euthanasia: loss of 20% of BW and/or absence of exploratory behavior, loss of relative immobility, or failure to groom.

### **Intraperitoneal glucose and insulin tolerance tests**

For the intraperitoneal glucose tolerance test (IPGTT), mice were denied access to food overnight (16–18 h); thereafter, glucose was administered at 2 mg/g BW. Blood glucose values

were determined (Accu-Chek Advantage II; Roche Diagnostics, Mannheim, Germany) before injection and at specific time points thereafter. For the intraperitoneal insulin tolerance test (IPITT), soluble insulin (0.5 mU/g BW; Actrapid; Novo Nordisk, Baulkham Hills, NSW, Australia) was administered after 6 h of food withdrawal (38).

### Serum and pancreatic hormone measurements

Serum was separated from whole blood, and pancreatic extracts were prepared from snap-frozen tissues obtained from animals in the different stages of diabetes by using the acid/ethanol method (38). Total pancreatic protein concentrations were determined by BCA assay (Pierce Biotechnology, Rockford, IL, USA). Serum and pancreatic levels of mouse insulin (Linco Research, St. Charles, MO, USA), hA (Linco Research), total amylin (Peninsula Laboratories, San Carlos, CA, USA), and glucagon (Yanaiharu Institute, Inc., Shizuoka, Japan) were measured by ELISA, RIA, or EIA, per the respective manufacturers' instructions. The sequences of rat amylin and mouse amylin are identical: here, the abbreviation mA has been used for this molecule, since these experiments were all performed in mice.

### Immunofluorescence staining

Pancreatic tissues were harvested at various time points corresponding to the different diabetic stages. Tissues were immediately fixed in formalin, or embedded in optimal cutting temperature (OCT) compound (Sakura Finetek, Torrance, CA, USA), and stored frozen at  $-80^{\circ}\text{C}$ . After antigen retrieval, 7  $\mu\text{m}$  sections were blocked with 10% normal donkey serum in PBS for 2 h before incubation with specific primary antibodies for insulin (Dako, Carpinteria, CA, USA), hA (Peninsula Laboratories), or cleaved caspase-3 (Cell Signaling, Danvers, MA, USA). For staining of hA oligomers, tissue sections were permeabilized with  $\text{H}_2\text{O}_2$  and methanol and underwent antigen retrieval by boiling (water bath, 30 min), to allow detection of intracellular and extracellular amylin oligomer-like immunoreactive material (AOLIM), performed according to the manufacturer's protocol with an oligomer-specific antibody (A11; Chemicon, Billerica, MA, USA). Note that the signals generated by this procedure have been designated as AOLIM, to reflect ongoing uncertainties about the exact structures of the species identified by this antibody. Appropriate FITC- or rhodamine red-conjugated secondary antibodies (Jackson ImmunoResearch, West Grove, PA, USA) were then used for covisualization of the specific target proteins. Stained sections were examined and imaging was performed by fluorescence microscopy (Axioskop 2 Plus; Zeiss, Jena, Germany). At least 4 islets/section, 3

sections/mouse, and 4 mice/group were examined. The specificity of immunofluorescence signals was confirmed by preincubation of each antibody used, with a 5–10 fold excess of the corresponding antigen solution (results not shown).

### Reverse transcription-qPCR (RT-qPCR) analysis

Total RNA was extracted from the pancreas by using an RNeasy mini kit (Qiagen, Tübingen, Germany), and cDNA was prepared with a Transcriptor First Strand cDNA Synthesis kit (Roche Applied Science). RT-qPCR was then performed with LC480 SYBR Green-I MasterMix on an LC480 LightCycler System (Roche Applied Science), and data were analyzed using the relative quantification method, as described in the manufacturer's instruction manual. qPCR data were normalized to the geometric mean of the optimal reference genes (*Ppia*, *Gapdh*, *Hprt1*, and *U2af*), evaluated as described in the minimum information for publication of quantitative real-time PCR experiments (MIQE) guidelines (42). The qPCR primers used are shown in Table 1.

### Quantitative histomorphometry

Pancreatic sections were stained with hematoxylin and eosin, and cross-sectional islet areas and total pancreatic areas were determined by light microscopy with image analysis software (Axio-Vision 2; Zeiss).  $\beta$ -Cell mass was estimated according to the method of Bonner-Weir (38, 43), based on the total pancreatic weight and relative volume (derived from percentage islet area) of the  $\beta$  cells, wherein the pancreatic weight is equated to pancreatic volume under the reasonable assumption that 1  $\text{cm}^3$  tissue weighs 1 g.

The percentage of islet area occupied by oligomer staining was determined by fluorescence microscopy, and ImageJ software (U.S. National Institutes of Health, Bethesda, MD, USA, USA; <http://rsbweb.nih.gov/ij/>) was used to analyze immunofluorescence-stained sections labeled with a widely used, oligomer-specific antibody (A11; Chemicon). At least 4 islets/section, 2 sections/mouse, and 4 mice/group were examined.

### Statistical analysis

All data are presented as means  $\pm$  SEM. Differences between experimental groups were analyzed with the unpaired, 2-tailed Student's *t* test or ANOVA (Prism 5; GraphPad, San Diego, CA, USA), with *post hoc* tests as appropriate and significance set at  $P < 0.05$ . Correlation analysis was performed to calculate the correlation coefficient (*r*) and *P* values.

TABLE 1. Sequences of primers used for the RT-qPCR analysis

Gene	Symbol	Forward/reverse sequences, 5'–3'
Insulin-1	<i>Ins1</i>	ccacaagtggaaacaactgga/gtgcagcactgatccacaat
Insulin-2	<i>Ins2</i>	ggagcgtggcttcttctaca/cagtgccaaaggtctgaaggt
Mouse amylin	<i>Iapp</i>	catgcagacttgggctgtagt/cagtgccacagagaggatga
Glucose transporter 2	<i>Glut2</i>	ggaagaggcatcgactga/ctaagggctgggggttactg
Glucokinase	<i>Gck</i>	gagccgcactggctctctg/actctgggacctctatcctctg
Peptidylprolyl isomerase A	<i>Ppia</i>	cgcgtctcctctcgagctgtttg/tgtaaagtcaccaccctggca
Glyceraldehydes-3-phosphate dehydrogenase	<i>Gapdh</i>	tgacgtgccgctggagaaa/agtgtagcccaagatgcccttcag
Hypoxanthine guanine phosphoribosyl transferase 1	<i>Hprt1</i>	gcttgctgggtgaaaaggacctctcgaag/ccctgaagtaactcattatagtcaggggcat
U2 auxiliary factor 36 kDa subunit	<i>U2af</i>	ccattgccctcttgaacatt/cttccccgtaacttctcttcc



## RESULTS

### Impaired glucose tolerance and altered insulin responsiveness occur before the onset of diabetes in homozygous hA-transgenic mice

The homozygous L13 hA-transgenic mice developed diabetes as early as 24 d of age (Fig. 1A); by contrast, the hemizygous mice developed diabetes only after they had become adults, consistent with prior reports (38, 39). The IPGTT performed during the early-stage diabetes period revealed fasting blood hyperglycemia compared with the nontransgenic littermate controls (homo,  $7.4 \pm 1.0$  vs.  $4.1 \pm 0.5$  mM,  $P < 0.01$ ; hemi,  $7.8 \pm 0.9$  vs.  $4.8 \pm 0.6$  mM;  $P < 0.01$ ;  $n = 10$ /group) and impaired glucose tolerance (IGT) in both the homozygous and hemizygous animals (Fig. 1B). The homozygous mice had serum and pancreatic insulin levels equivalent to control values in the nontransgenic littermates in the early stage of disease development (Tables 2 and 3). By contrast, the hemizygous mice showed significant decreases in insulin levels, as compared to their age-matched, nontransgenic control littermates, consistent with impaired  $\beta$ -cell function. In addition, IPGTT during the prediabetic stage (before disease onset) also demonstrated IGT in both the homozygous and hemizygous mice (Fig. 1C). However, fasting blood insulin values were increased during IPGTT in the homozygous animals compared with those in the nontransgenic controls ( $t_0$   $61.2 \pm 12.6$  vs.  $29.2 \pm 9.6$  pM;  $P < 0.01$ ;  $n = 9$ /group), whereas the hemizygous mice retained normal fasting blood insulin levels equivalent to those in the age-matched controls

during the prediabetic stage ( $t_0$   $62.4 \pm 13.6$  vs.  $76.8 \pm 19.4$  pM;  $P =$  not significant;  $n = 10$ /group). The presence of elevated levels of fasting and nonfasting circulating insulin (Table 2) in the presence of IGT in the homozygous mice was consistent with insulin resistance in these animals. There were thus important differences in insulin responses between the homozygous and hemizygous mice during the prediabetes stage.

Furthermore, IPITT in the hemizygous mice during the prediabetes stage (Fig. 1D) demonstrated sensitive systemic responses to insulin, consistent with the absence of insulin resistance, as we have reported (38). By contrast, homozygous mice were clearly less responsive to insulin administration during the IPITT (Fig. 1E), consistent with decreased insulin sensitivity. These results indicate that insulin resistance may be a significant pathogenic factor in the triggering of diabetes in homozygous L13 mice. Thus, the homozygous animals develop early-onset diabetes through mechanisms that differ in significant respects from the mechanisms of its development in adult hemizygous animals of the same transgenic line.

### hA oligomerization and its correlation with pancreatic hA levels

We have determined by qPCR that individual homozygous hA-transgenic mice (L13) possess  $74 \pm 4$  copies of the transgene, whereas corresponding hemizygous individuals have  $36 \pm 7$ , as previously reported (39). In the current study, serum and pancreatic levels of hA in the homozygous mice in prediabetes and early diabetes were generally about

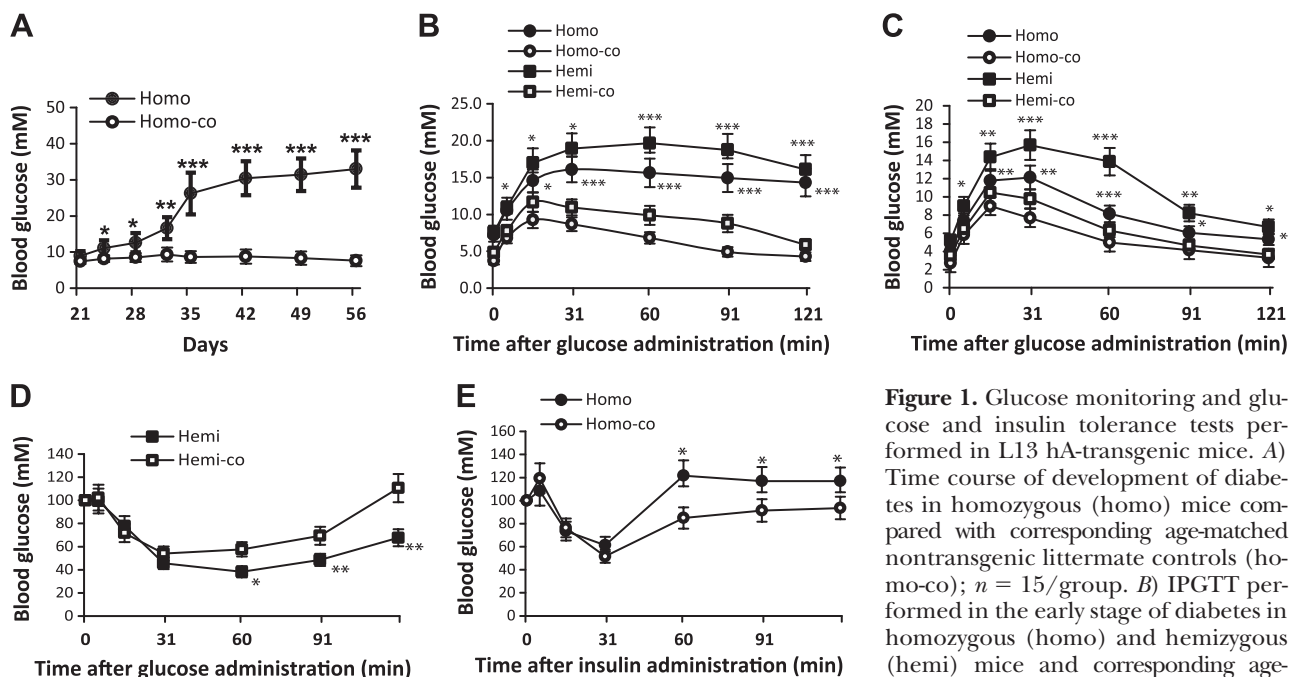


**Figure 1.** Glucose monitoring and glucose and insulin tolerance tests performed in L13 hA-transgenic mice. A) Time course of development of diabetes in homozygous (homo) mice compared with corresponding age-matched nontransgenic littermate controls (homo-co);  $n = 15$ /group. B) IPGTT performed in the early stage of diabetes in homozygous (homo) and hemizygous (hemi) mice and corresponding age-matched nontransgenic littermate controls (homo-co or hemi-co, respectively);  $n = 10$ –12/group. C) IPGTT performed in the prediabetic stage;  $n = 10$ –12/group. D) IPITT in the prediabetic stage in hemizygous mice and corresponding age-matched nontransgenic controls ( $n = 10$ /group). E) IPITT in the prediabetic stage in homozygous and corresponding age-matched nontransgenic controls ( $n = 10$ /group). All values are means  $\pm$  SEM. \* $P < 0.05$ , \*\* $P < 0.01$ , \*\*\* $P < 0.001$  vs. nontransgenic controls.

controls (homo-co or hemi-co, respectively;  $n = 10$ –12/group). C) IPGTT performed in the prediabetic stage;  $n = 10$ –12/group. D) IPITT in the prediabetic stage in hemizygous mice and corresponding age-matched nontransgenic controls ( $n = 10$ /group). E) IPITT in the prediabetic stage in homozygous and corresponding age-matched nontransgenic controls ( $n = 10$ /group). All values are means  $\pm$  SEM. \* $P < 0.05$ , \*\* $P < 0.01$ , \*\*\* $P < 0.001$  vs. nontransgenic controls.

TABLE 2. Serum levels of pancreatic hormones in prediabetes and early-, mid-, late- and end-stage diabetes in L13 homozygous and hemizygous hA-transgenic and corresponding age-matched nontransgenic control mice

Parameter	Prediabetes	Early-stage	Mid-stage	Late-stage	End-stage
Homozygous/homo-co					
Age (d)	23 ± 2	27 ± 3	32 ± 3	40 ± 4	55 ± 6
Blood glucose (mM)					
Homozygous	10.1 ± 0.6**	12.3 ± 0.9***	19.8 ± 1.3***	29.6 ± 1.4***	> 33.0
Homo-co	8.2 ± 0.6	8.8 ± 1.1	9.2 ± 1.2	8.6 ± 0.9	9.1 ± 1.1
Body weight (g)					
Homozygous	9.8 ± 0.31	17.7 ± 0.33	21.1 ± 0.34	20.9 ± 0.56**	16.8 ± 0.99***
Homo-co	10.3 ± 0.41	18.1 ± 0.51	22.7 ± 0.42	24.6 ± 0.55	26.7 ± 1.02
Insulin					
Homozygous	133.1 ± 14.6**	97.9 ± 8.8	83.9 ± 8.2**	63.4 ± 8.7***	62.2 ± 8.4***
Homo-co	68.44 ± 5.9	88.0 ± 6.9	147.3 ± 15.7	153.6 ± 18.8	278.4 ± 31.2
Human amylin					
Homozygous	5.8 ± 0.8 <sup>+++</sup>	6.0 ± 0.5 <sup>+++</sup>	2.7 ± 0.5	0.7 ± 0.1	ND
Homo-co	ND	ND	ND	ND	ND
Total amylin					
Homozygous	27.8 ± 3.8***	33.0 ± 4.5***	11.8 ± 2.2***	5.1 ± 0.6	2.9 ± 0.4**
Homo-co	4.1 ± 0.3	5.3 ± 0.6	4.5 ± 1.1	4.5 ± 0.5	4.8 ± 0.5
Mouse amylin					
Homozygous	22.0 ± 4.6***	27.0 ± 5.0***	9.1 ± 2.7***	4.4 ± 0.7	2.9 ± 0.4**
Homo-co	4.1 ± 0.3	5.3 ± 0.6	4.5 ± 1.1	4.5 ± 0.5	4.8 ± 0.5
Glucagon					
Homozygous	107.5 ± 12.6	101.5 ± 13.2	97.3 ± 12.1	109.3 ± 15.5	165.4 ± 20.3**
Homo-co	100.3 ± 13.4	93.3 ± 11.1	124.7 ± 18.2	87.4 ± 96.7	78.3 ± 9.8
Hemizygous/hemi-co					
Age (d)	72 ± 11	105 ± 26	156 ± 39	215 ± 48	310 ± 61
Blood glucose (mM)					
Hemizygous	9.8 ± 0.5*	12.9 ± 0.8***	20.1 ± 1.7***	29.2 ± 1.0***	> 33.0
Hemi-co	7.9 ± 0.9	8.6 ± 1.2	8.3 ± 0.7	8.4 ± 0.9	9.2 ± 1.2
Body weight (g)					
Hemizygous	28.9 ± 0.61*	31.4 ± 0.47*	32.0 ± 0.55	30.5 ± 0.45	25.1 ± 1.2***
Hemi-co	26.2 ± 1.2	28.9 ± 1.1	29.4 ± 0.96	29.6 ± 0.95	33.6 ± 1.3
Insulin					
Hemizygous	100.8 ± 23.6	184.0 ± 37.6**	185.7 ± 35.8**	82.2 ± 21.5**	47.7 ± 13.2***
Hemi-co	192.6 ± 41.6	373.6 ± 47.8	297.7 ± 60.4	230.3 ± 31.8	340.6 ± 59.3
Human amylin					
Hemizygous	2.30 ± 0.3	3.05 ± 0.7	2.24 ± 0.43	0.85 ± 0.11	ND
Hemi-co	ND	ND	ND	ND	ND
Total amylin					
Hemizygous	25.2 ± 5.1***	41.4 ± 4.0***	29.5 ± 5.5***	15.4 ± 1.3	7.3 ± 1.6***
Hemi-co	14.3 ± 2.5	9.4 ± 0.9	11.6 ± 1.2	15.5 ± 1.0	14.6 ± 2.0
Mouse amylin					
Hemizygous	22.9 ± 5.3***	38.3 ± 4.7***	27.2 ± 5.8**	14.5 ± 1.4	7.3 ± 3.6***
Hemi-co	14.3 ± 2.5	9.4 ± 0.9	11.6 ± 1.2	15.5 ± 1.0	14.6 ± 2.0
Glucagon					
Hemizygous	133.0 ± 18.5	94.4 ± 11.8	89.8 ± 11.6	109.8 ± 16.2	127.2 ± 17.8**
Hemi-co	162.9 ± 20.9	99.8 ± 13.1	105.1 ± 14.6	122.2 ± 19.9	86.1 ± 13.2

Male animals were used in all experiments. Hormone levels are means ± SE (pM). Levels of mA were determined by subtraction of hA from total amylin (hA+mA). Homo-co, homozygous control; hemi-co, hemizygous control; ND, not detected. \* $P < 0.05$ , \*\* $P < 0.01$ , \*\*\* $P < 0.001$  vs. nontransgenic control; <sup>+++</sup> $P < 0.001$  vs. hemizygous mice ( $n = 8-10$ ).

2-fold higher than those in the hemizygous mice at the comparable disease stages, although the homozygous mice were much younger in chronological age (Tables 2 and 3). By the mid-diabetes stage, however, hA levels had decreased to equivalent values, and they subsequently fell to lower levels during the late-diabetes stage. These results are consistent with the immunohistochemical evidence (Fig. 2A, B), which showed a rapid loss of hA-positive islet cells during disease progression in the homozygous mice.

hA was unmeasurable in the end-stage mice and in the nontransgenic control mice at any stage (Fig. 2C).

We next asked whether hA oligomers might form *in vivo* and how this process might correlate with the levels of hA expression as diabetes progressed. In double-immunofluorescence studies (Fig. 2), performed using antibodies specific for oligomeric hA (24, 44), all (that is, with 100% frequency) transgenic islets displayed signs of oligomer formation. This signal is herein

TABLE 3. Pancreatic hormone levels in the various stages of diabetes in L13 homozygous and hemizygous hA-transgenic and corresponding age-matched nontransgenic control mice

Parameter	Prediabetes	Early-stage	Mid-stage	Late-stage	End-stage
<b>Insulin</b>					
Homozygous	7.79 ± 0.87**	5.57 ± 0.67	2.25 ± 0.33**	0.38 ± 0.06***	0.33 ± 0.06***
Homo-co	4.21 ± 0.64	6.44 ± 0.83	5.98 ± 0.72	4.91 ± 0.76	4.65 ± 0.68
<b>Human amylin</b>					
Homozygous	0.65 ± 0.08 <sup>2+</sup>	0.90 ± 0.12 <sup>+++</sup>	0.27 ± 0.03	0.08 ± 0.01	ND
Homo-co	ND	ND	ND	ND	ND
<b>Total amylin</b>					
Homozygous	2.12 ± 0.22***	1.87 ± 0.21**	0.98 ± 0.12*	0.32 ± 0.06*	0.11 ± 0.03***
Homo-co	0.25 ± 0.03	0.27 ± 0.03	0.38 ± 0.05	0.44 ± 0.06	0.34 ± 0.05
<b>Mouse amylin</b>					
Homozygous	1.47 ± 0.30**	0.97 ± 0.33**	0.71 ± 0.15**	0.24 ± 0.07***	0.11 ± 0.03***
Homo-co	0.25 ± 0.03	0.27 ± 0.03	0.38 ± 0.05	0.40 ± 0.06	0.34 ± 0.05
<b>Glucagon</b>					
Homozygous	1.67 ± 0.21	0.89 ± 0.12	0.82 ± 0.13	1.00 ± 0.38	1.18 ± 0.24
Homo-co	1.78 ± 0.22	1.02 ± 0.18	1.17 ± 0.21	1.68 ± 0.36	1.03 ± 0.19
<b>Insulin</b>					
Hemizygous	4.61 ± 1.01	2.82 ± 0.19*	1.22 ± 0.28**	0.56 ± 0.11***	0.23 ± 0.05***
Hemi-co	3.65 ± 0.51	4.62 ± 0.56	5.44 ± 1.07	6.70 ± 0.86	5.52 ± 0.64
<b>Human amylin</b>					
Hemizygous	0.36 ± 0.06	0.46 ± 0.06	0.20 ± 0.04	0.04 ± 0.005	ND
Hemi-co	ND	ND	ND	ND	ND
<b>Total amylin</b>					
Hemizygous	2.61 ± 0.35*	2.56 ± 0.37**	1.59 ± 0.21*	0.46 ± 0.11**	0.20 ± 0.04***
Hemi-co	0.30 ± 0.05	0.38 ± 0.06	0.45 ± 0.05	0.51 ± 0.12	0.48 ± 0.07
<b>Mouse amylin</b>					
Hemizygous	2.25 ± 0.41*	2.10 ± 0.42**	1.39 ± 0.25	0.42 ± 0.12**	0.20 ± 0.04***
Hemi-co	0.30 ± 0.05	0.38 ± 0.06	0.45 ± 0.05	0.51 ± 0.12	0.48 ± 0.07
<b>Glucagon</b>					
Hemizygous	0.78 ± 0.11	0.65 ± 0.11	0.45 ± 0.07*	0.90 ± 0.21	1.06 ± 0.39
Hemi-co	0.65 ± 0.09	0.69 ± 0.12	1.07 ± 0.18	1.25 ± 0.20	1.70 ± 0.26

BW and age were as shown in Table 2. Data are means ± SE. Hormone levels (ng/mg pancreas) were normalized to pancreatic wet weight. Levels of mA were determined by subtraction of hA from total amylin (hA+mA). Homo-co, homozygous control; hemi-co, hemizygous control; ND, not detected. \* $P < 0.05$ , \*\* $P < 0.01$ , \*\*\* $P < 0.001$  vs. nontransgenic control mice. <sup>++</sup> $P < 0.01$ , <sup>+++</sup> $P < 0.001$  vs. hemizygous mice ( $n=8-10$ ).

designated AOLIM, to differentiate it from that due to hA in its nonmisfolded, physiological conformation. Islet morphometric analysis showed that a maximum amount of ~30–40% of total islet area displayed AOLIM (Fig. 3A) and that it was associated with higher levels of pancreatic hA in prediabetes and early diabetes in homozygous mice (Figs. 2A and 3B). By contrast, AOLIM was densest during mid- and late-stage diabetes in hemizygous mice (Figs. 2B and 3A), when pancreatic hA levels had already declined, indicating that the extent of AOLIM did not correlate positively with hA levels in the hemizygous animals (instead, it was inversely correlated; Fig. 3C). These results may point to different roles of AOLIM during pathogenesis in the homozygous and hemizygous animals. In addition, no AOLIM was detected in the islets of any of the nontransgenic mice (Fig. 2C), indicating that the anti-oligomer antibody detects a signal that is present only in transgenic islets; moreover, preincubation of this antibody with a preparation of hA oligomers (prepared as described in ref. 27) completely abolished the AOLIM signal (data not shown), consistent with the specificity of this antibody for hA oligomers, as opposed to nonaggregated hA.

Notably, levels of endogenous mA in the homozygous mice were significantly higher (2–5-fold) than in

the littermate controls during prediabetes and early-stage diabetes (Tables 2 and 3), consistent with previous findings in the hemizygous animals (38). In addition, increased circulating glucagon levels were present in both the homozygous and hemizygous mice but only during their respective end-diabetes stages (Table 2), whereas by contrast, pancreatic glucagon levels remained equivalent to nondiabetic control values at all disease stages (Table 3). Thus hyperglucagonemia is a manifestation of end-stage diabetes syndromes in both homozygous and hemizygous hA-transgenic mice, which occurs as a result of diabetes and is thus not causal thereof.

### Role of hA oligomerization in $\beta$ -cell dysfunction and impaired insulin responses

Since the time at which AOLIM staining increased did not necessarily correlate with the highest levels of hA expression, we examined the correlation between AOLIM and insulin expression (Fig. 4). AOLIM correlated with pancreatic insulin levels, as it did with hA levels. Almost all the AOLIM signal was localized within or adjacent to insulin-positive cells, and dense AOLIM was present during the hyperinsulinemic phase in the prediabetic homozygous mice (Fig. 4A), whereas the

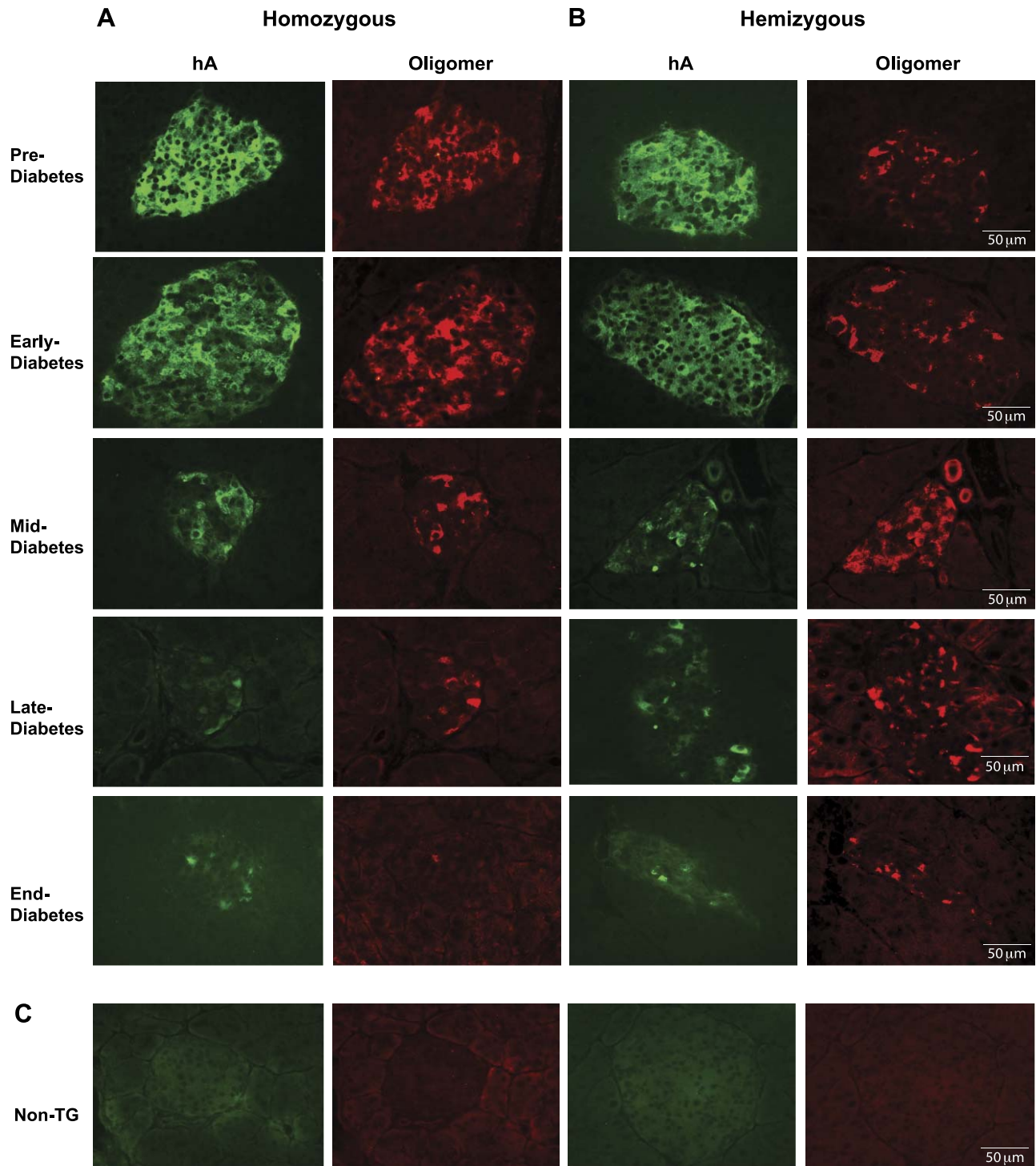


**Figure 2.** Representative double-immunofluorescence staining for pancreatic islet hA (green) and AOLIM (red) in hA-transgenic prediabetic mice and those in the various stages of diabetes. A) hA and AOLIM were detected in homozygous mice. B) hA and AOLIM were detected in hemizygous mice. C) Neither hA nor AOLIM was detected in the nontransgenic islets, as demonstrated by a representative study in the early stage. Data are representative of  $\geq 4$  islets/section, 2 sections/mouse, and 4 mice/group. Scale bars = 50  $\mu\text{m}$ .

maximum AOLIM staining in the hemizygous mice was associated with lowered insulin levels during mid- and late-stage diabetes (Figs. 4B and 5A).

We next studied the correlation of hA levels with  $\beta$ -cell dysfunction, as shown by alterations in glucose responses and insulin expression. Double-immunofluorescence staining demonstrated that hA-positive cells

were mostly insulin-producing  $\beta$  cells, with two discernible populations displaying apparently different intensities of insulin staining (Fig. 5B). Densely insulin-stained cells were more abundant in the homozygous animals during prediabetes. Both serum and pancreatic insulin levels declined markedly, along with hA hormone levels, during the later stages of disease progres-



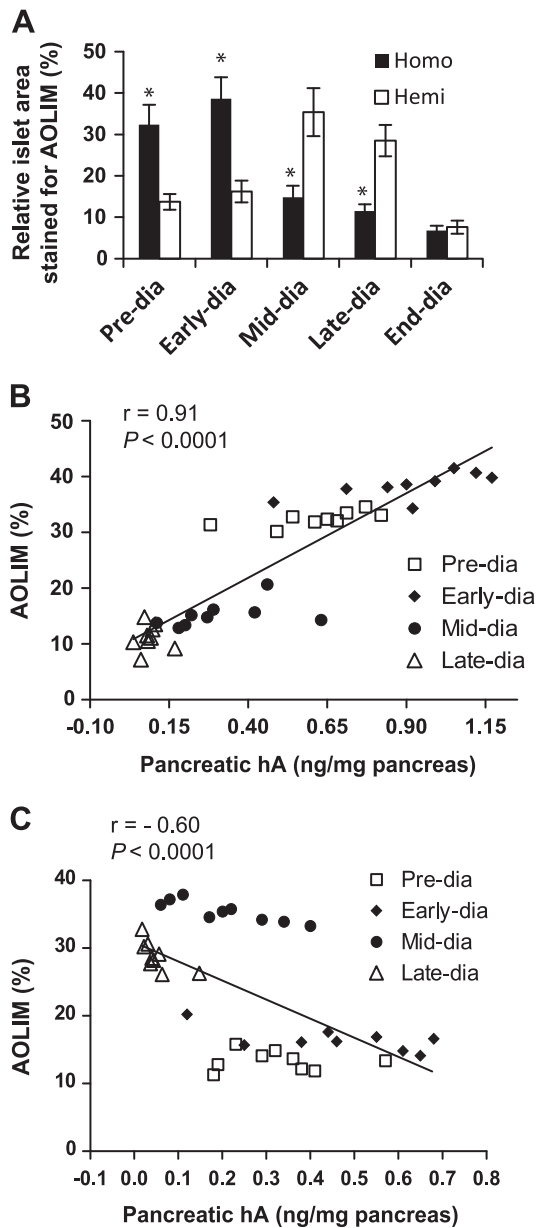


**Figure 3.** Severity of hA oligomer formation and its correlation with pancreatic hormone levels. *A*) Percentage of islet area stained with AOLIM was estimated by quantifying the AOLIM-positive area within each islet by using ImageJ software. At least 4 islets/section, 2 sections/mouse, and 4 mice/group were examined. Results are means  $\pm$  SEM.  $*P < 0.05$ . *B*) Correlation of AOLIM with pancreatic hA levels in homozygous mice. *C*) Correlation of AOLIM with pancreatic hA levels in hemizygous mice. Correlation coefficients ( $r$ ) and  $P$  values, the latter indicating whether slopes are significantly different from 0, are as stated in each graph (*B*, *C*;  $n=9$ /group).

sion, consistent with the ongoing disappearance of hA-positive  $\beta$  cells. These results are consistent with correlation analyses showing that serum insulin levels correlated well with serum hA and mA levels in the homozygous and hemizygous mice in the different disease stages (Fig. 4C–F).

Analysis by RT-qPCR of the expression of  $\beta$ -cell-specific genes at the time of diabetes onset in the

hemizygous mice showed significant decreases in islet mRNA levels corresponding to insulin 1 (*Ins1*), insulin 2 (*Ins2*), mA (*Iapp*), glucose transporter 2 (*Glut2*), and glucokinase (*Gck*) (Fig. 6A), indicating deficient mRNA expression of  $\beta$ -cell hormones and glucose-responsive genes from the  $\beta$ -cell secretory pathway. By contrast, mRNA levels of all these genes were not different from the control values in homozygous islets at the comparable stage (Fig. 6B).

### Temporal correlation of amylin oligomerization with $\beta$ -cell death and disease onset

We compared the time at which the maximum hA oligomerization occurred in the islets of transgenic mice to the timing of diabetes onset and signs of  $\beta$ -cell death.  $\beta$ -Cell death by apoptosis was detected by double-immunofluorescence staining of active caspase-3 with insulin or AOLIM (Fig. 7). Active caspase-3 was colocalized to the cell bodies of insulin-positive cells (Fig. 7A), indicating that apoptosis occurred selectively in insulin-containing  $\beta$  cells. Furthermore, active caspase-3 was detectable during the prediabetic stage in the homozygous mice (Fig. 7B), mostly correlating with the peak time of occurrence of hA oligomerization (Fig. 3A). In the hemizygous mice, active caspase-3 was not detected during early-stage diabetes, but was increased during the mid and late stages, when AOLIM was abundant (Fig. 7B). This finding also correlated with the peak time occurrence of hA oligomerization in the hemizygous animals (Fig. 3A) and is consistent with the idea that AOLIM formation could contribute mainly to the  $\beta$ -cell death and disappearance occurring in the islets during the development of diabetes.

To further elucidate the mechanisms of  $\beta$ -cell death *in vivo* and possible roles of hA oligomerization, we also performed quantitative histomorphometry to measure islet  $\beta$ -cell mass at different stages of disease. Figure 8 shows that there was a significant decrease in  $\beta$ -cell mass soon after disease onset in the homozygous mice (Fig. 8A); by contrast, an equivalent decline did not occur until after mid-stage diabetes in the hemizygous mice (Fig. 8B).

### DISCUSSION

Spontaneous diabetes develops in hemizygous hA-transgenic mice (L13) through a mechanism that appears to be independent of insulin resistance and the presence of islet amyloid (38, 39). We report our detailed phenotypic characterization of homozygous hA-transgenic mice, by comparison and contrast with corresponding hemizygous mice from the same line regarding hormonal responses, hA oligomerization, islet  $\beta$ -cell function, and disease onset and progression. We show that overexpression of hA in juvenile homozygous mice leads to or causes glucose intolerance and diminished insulin sensitivity associated with concomitantly increased basal and fasting insulin levels in the prediabetic stage, consistent with the presence of insulin resistance that was, however, self-limited by the rapid



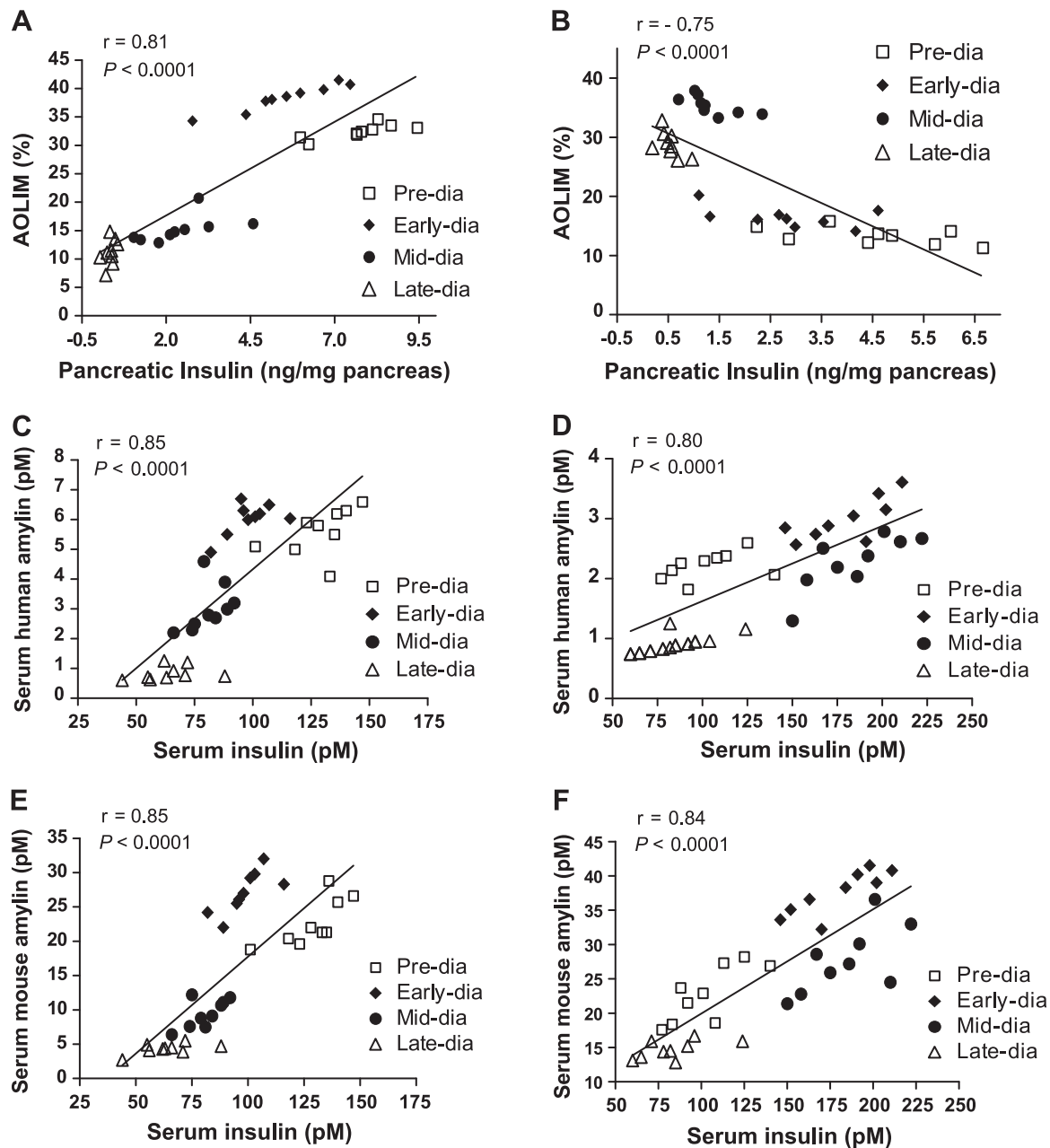


**Figure 4.** Correlation analyses of AOLIM with pancreatic insulin levels in homozygous (A) and hemizygous (B) mice; serum insulin with hA levels in homozygous (C) and hemizygous (D) mice; and serum insulin and mA levels in homozygous (E) and hemizygous (F) mice. Correlation coefficients ( $r$ ) and  $P$  values, the latter indicating whether slopes are significantly different from 0, are stated in each graph ( $n=9$ /group).

and progressive  $\beta$ -cell disappearance that followed shortly thereafter.

The resulting phenotype, which was present at the time of diabetes onset in the homozygous mice, appears to be consistent with that of type 1 diabetes, for example, in the group of patients who do not develop detectable insulinitis (45). We therefore postulate that hA misfolding acts as a trigger for the initiation of  $\beta$ -cell destruction in such patients, since the ongoing release of amylin from residual  $\beta$  cells (which are amylin as well as insulin secreting) must occur, thereby providing a localized autocrine cytotoxic stimulus. However, to our knowledge, the possibility that hA acts as such a trigger in type 1 diabetes has not been investigated. By con-

trast, prediabetic hemizygous mice are typically more insulin responsive and exhibit normal rates of insulin-stimulated glucose uptake in *ex vivo* skeletal muscle preparations (38). The molecular explanation for greater insulin responsiveness during the IPITT in the hemizygous animals remains to be further investigated. It is possible that increased insulin responsiveness compensates for decreased insulin levels and impaired  $\beta$ -cell function (*i.e.*, defective glucose-stimulated insulin secretion) as indicated by RT-qPCR analysis showing decreased pancreatic mRNA levels of *Ins1*, *Ins2*, *Iapp*, *Glut2*, and *Gck*. Thus, the prediabetic stage in the homozygous L13 mice differed substantively from the equivalent stage in the hemizygous animals. The higher

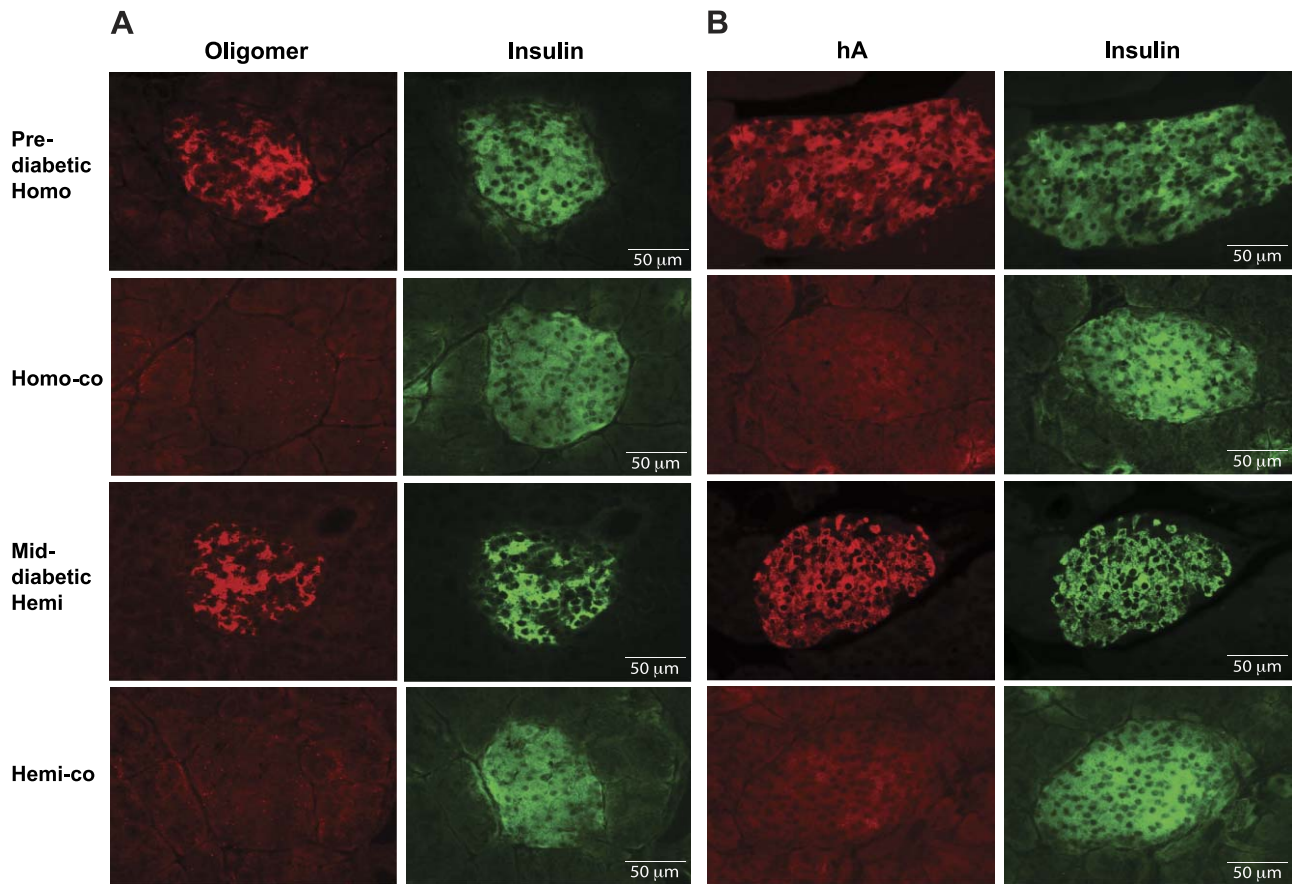


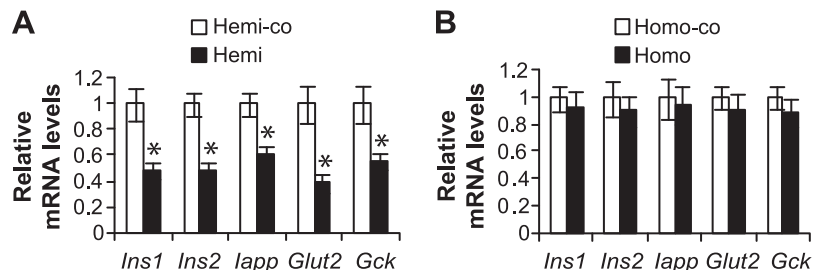
**Figure 5.** Representative double-immunofluorescence staining for insulin (green) and AOLIM (red; A) or hA (red; B), in which  $\geq 30$  islets were examined from homozygous and hemizygous hA-transgenic mice and corresponding age-matched, nontransgenic controls (homo-co and hemi-co, respectively), in prediabetes and mid-stage diabetes. Neither hA nor AOLIM was detected in nontransgenic control islets. Data are representative of  $\geq 4$  islets/section, 2 sections/mouse, and 4 mice/group. Scale bars = 50  $\mu\text{m}$ .

levels of hA produced in the homozygous mice before disease onset and during the early diabetic stage were most likely due to the higher copy number of the transgene in the homozygous animals, so these findings are consistent with a gene-dosage effect. Hyperamylinemia induced by hA overexpression is accompanied by hyperinsulinemia in the prediabetic stage, which could contribute to the development of insulin resistance. We have therefore demonstrated fundamental differences in the pathogenesis of diabetes caused by the variance in levels of elevation of hA between the two genotypes.

Different strains of hA-transgenic mice have been constructed by several groups, and each strain exhibits particular phenotypic characteristics (15, 34, 35, 38, 39, 46, 47). The differences in genetic backgrounds of

these different models, taken together with possible genetic background–transgene interactions and differences in hA transgene expression, could account for the between-model phenotypic variation that has been reported (14, 38). Our hemizygous mice reported here may be closest to the homozygous mice reported by Janson *et al.* (15). We found no evidence of Congo red–detectable, large, mature islet amyloid deposits in any of the homozygous transgenic mice at any stage (data not shown). This finding further supports the view that large, mature amyloid deposits *per se* are not necessary for the development of  $\beta$ -cell degeneration and diabetes. Instead, currently available results point to small, soluble oligomers as the probable cytotoxic forms of hA, since such oligomers (mea-

**Figure 6.** RT-qPCR analysis of pancreatic mRNA levels of *Ins1*, *Ins2*, *Iapp*, *Glut2*, and *Gck* in early-stage hemizygous (A) and homozygous (B) diabetic mice. Results were normalized to a robust standard (geometric mean of mRNA levels of *Ppia*, *Gapdh*, *Hprt1*, and *U2af*) and are presented relative to corresponding nontransgenic control values, which were set at 1. Results are means  $\pm$  SEM of 3 independent experiments, each performed in triplicate. \* $P < 0.01$  vs. nontransgenic controls.



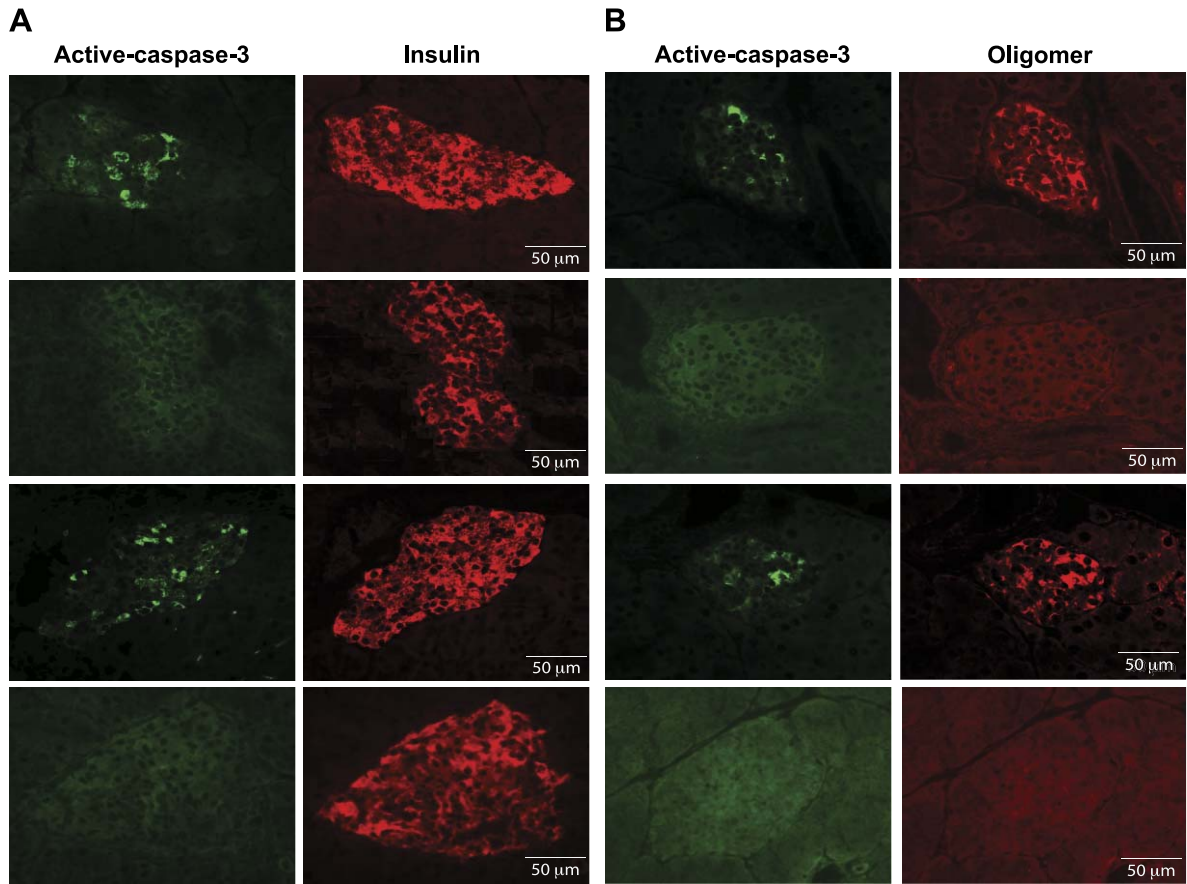


**Figure 7.** Representative double-immunofluorescence staining of active caspase-3 (green) and insulin (red; A) or AOLIM (red; B), in which  $\geq 30$  islets were examined from homozygous and hemizygous hA-transgenic mice and their corresponding matched controls (homo-co and hemi-co, respectively) in early- and mid-stage diabetes. No AOLIM or active caspase-3 cells were detected in nontransgenic islets. Data are representative of  $\geq 4$  islets/section, 2 sections/mouse, and 4 mice/group. Scale bars = 50  $\mu\text{m}$ .

sured as AOLIM) were clearly detectable in the islets of both the homozygous and hemizygous mice. This evidence was strengthened by our demonstration that AOLIM positivity was abrogated by pretreatment of AOLIM antibodies with an hA-oligomer-containing solution.

The oligomer-specific antibody used in the current study was raised against a preparation containing toxic  $\text{A}\beta_{1-40}$  oligomers (15, 24, 44). This antibody is widely said to recognize misfolded tertiary structural properties shared in common by several pathogenetic amyloid monomers, including hA,  $\text{A}\beta_{1-40}/\text{A}\beta_{1-42}$ ,  $\alpha$ -synuclein, transthyretin, and the scrapie prion protein  $\text{PrP}_{\text{SC}}$ , but does not recognize the monomers in their physiologi-

cal conformational states or the mature fibrillar forms of these peptides (44, 48). The specificity of this antibody to toxic hA oligomers has been evaluated by others (24, 28, 49), and it has also been reported to protect against hA-evoked cytotoxicity in cell culture systems, pointing to a mechanism mediated by an hA-cell membrane interaction (44). It has been used by others to detect the presence and location of hA oligomers in the islets of hA-transgenic mouse models of type 2 diabetes (24). Moreover, although it may cross-react with other misfolded ER/Golgi proteins, including  $\text{A}\beta$  in islet  $\beta$  cells, we detected no positive immunoreactive signals when we applied it in nontransgenic controls under our experimental conditions,

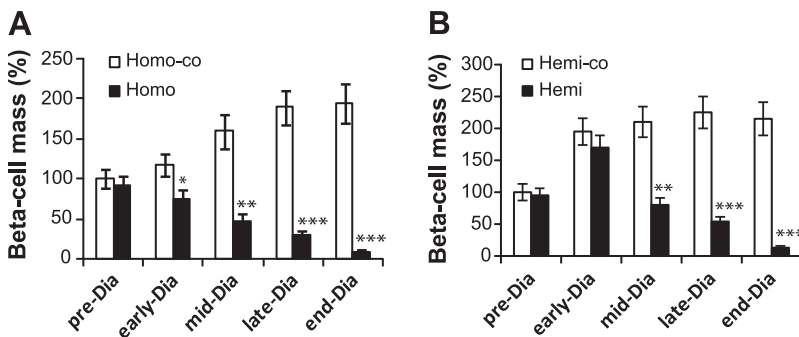


**Figure 8.** Quantitative analysis of  $\beta$ -cell mass in the islets of homozygous (A) and hemizygous (B) mice and corresponding nontransgenic controls (homo-co and hemi-co, respectively). The results are presented as percentage changes in  $\beta$ -cell mass in the prediabetes stage, relative to nontransgenic controls, whose mass was set at 100% ( $n=10$ ), \* $P < 0.05$ , \*\* $P < 0.01$ , \*\*\* $P < 0.001$  vs. nontransgenic controls.



thereby confirming that the AOLIM-positive signals are specific to hA-transgenic islets. The AOLIM detected in the current study may comprise various sizes and conformational states of aggregates of misfolded hA multimers with different cytotoxic potential, which could form in parallel with the different levels of hA transgene expression, as found in the homozygous and hemizygous mice. This possibility should be further examined.

In addition, it is interesting to note that, in the prediabetic hemizygous mice, levels of serum and pancreatic total amylin and mA were all increased, yet insulin was not significantly different from control values. However, mA was also increased in prediabetic homozygous mice where it was accompanied by increased insulin. The mechanism by which overexpression of hA leads to apparent increases in mA and the role this may have played in our transgenic model is not entirely clear, although it is evidently associated with increased insulin. The elevation of endogenous mA may contribute to the absence of islet amyloid, since mA has been reported to inhibit *in vitro* hA fibril formation (50), although direct evidence for such molecule–molecule interaction is not strong.

We further noted that AOLIM appeared not to accumulate or further assemble into large amyloid deposits, but rather that it seemed to be progressively cleared from affected islets, concomitant with  $\beta$ -cell disappearance and diabetes progression, indicating the likely existence of a clearance mechanism. Such clearance may be consistent with recent reports showing the presence of hA oligomers (particularly trimers, tetramers, octamers, and 16-mers) in the kidneys (51) and hearts (52) of patients with obesity or type 2 diabetes, as well as in hA-transgenic rats. These findings may indicate the clearance of hA oligomers from the pancreatic islets into the blood.

Transgenic mice overexpressing hA in their  $\beta$  cells could oversecrete hA and thus contribute to its misfolding, which in turn could lead to intra- and extracellular formation of oligomers that are cytotoxic to islet  $\beta$  cells, but not to other islet cell types. In the current study, longitudinal studies of hA oligomerization and  $\beta$ -cell death at different stages of diabetes development showed that the homozygous and hemizygous mice had different time frames from disease onset to death, which were differentially associated with elevated levels of hA transgene expression and the extent of hA oligomerization. The stage at which the maximum AOLIM occurred was different between the 2 genotypes, suggesting a separate mechanism by which hA oligomers contribute to diabetes onset and progression. Cross-sectional colocalization studies by multiple double-immunofluorescence staining for active caspase-3 with insulin, insulin with amylin, and amylin with AOLIM, showed that the time at which  $\beta$ -cell death became detectable coincided with maximum hA oligomer formation, indicating that extensive hA oligomerization could well be the direct cause of *in vivo*  $\beta$ -cell loss in the islets of this animal model, although the combined effects of high blood glucose could also contribute. Interestingly, AOLIM was detected in some but not all hA- or insulin-staining  $\beta$  cells, consistent

with previous reports (*e.g.*, ref. 24), but the underlying mechanisms for this nonuniform distribution remain obscure. Taken together, our findings imply that, although AOLIM associates mainly with the later progression of diabetes in hemizygous mice, it could contribute mainly during the stage of disease-triggering and onset in homozygous mice.

Studies using formalin-fixed autopsy samples have provided evidence of formation of hA oligomers and aggregates in the pancreatic islets of older patients with type 2 diabetes, as well as in nondiabetic individuals in whom hA oligomers were reportedly present, either as small, intracellular, spherical puncta or large, curvilinear, extracellular structures (49). However, it has not yet been possible to image the histopathologic changes that may occur during early development of type 1 and 2 diabetes in human islet tissue *in vivo*. Therefore, appropriately validated hA-transgenic models are the most practical and useful tools developed so far for preclinical investigation of the amylin-mediated pathogenesis of islet degeneration and for the modeling of possible pathogenetic mechanisms relevant to the development of experimental pharmacology for these human conditions. In this study, we characterized an hA-transgenic mouse model, wherein hemizygous mice may provide an accurate reflection of the corresponding disease process in adult patients with type 2 diabetes, and homozygous mice may provide a suitable model for studies of the triggering of juvenile-onset diabetes, which is currently increasing in incidence in many countries.

This work has limitations. For example, several major unanswered questions remain in the field of amylin in diabetes research, for which definitive answers are lacking and which have not been addressed by the work reported here. Is  $\beta$ -cell toxicity triggered in the intracellular or the extracellular space? Why is there a nonuniform distribution of amyloid and islet damage in the pancreases of patients with type 2 diabetes? What are the exact structures of the oligomers that cause  $\beta$ -cell damage and death, what are the molecular pathways that mediate this effect, and do these oligomers circulate in the blood? Why is amyloid deposited in much greater amounts in diabetic states than in nondiabetic, insulin-resistant states, in which large amounts of hA are secreted for decades without much evidence of damage from oligomers or amyloid deposition? Why does amyloid form in some insulinomas but not in others, and finally, does misfolding of amylin, an obligatory constituent of the islet  $\beta$ -cell granules that has the ability to form cytotoxic structures, contribute to the etiopathogenesis of type 1 diabetes, at least in some patient groups? Clearly, a great deal of work is needed before comprehensive answers to these very difficult questions are obtained. However, we think, based in part on the results of the current study, that these questions are of great significance for the understanding of the etiopathogenesis and development of experimental therapeutics for diabetes.

In summary, we have provided direct evidence of the existence of key variations in the diabetogenic processes that lead to the different time frames of diabetes onset and to progression in homozygous and hemizy-



gous hA-transgenic mice, wherein outcomes seem to depend on the levels of elevated hA expression as well as the resulting extent of hA oligomerization. AOLIM forms in islets before the occurrence of fasting hyperglycemia, so it appears that hA oligomers do not arise merely as a result of the diabetic state, but rather that they may well be causative thereof. The current findings seem to help reconcile the results of otherwise apparently divergent reports that have recently given rise to uncertainty concerning the cytotoxic mechanisms through which hA causes  $\beta$ -cell death and diabetes. This study provides strong support for the hypothesis that cytotoxic hA oligomers, acting dose dependently, play a pivotal role in the mechanism of  $\beta$ -cell destruction and that targeting the concomitant oligomerization pathway may have therapeutic potential in preventing or ameliorating degeneration and loss of  $\beta$  cells in diabetes. These findings have the potential to alter and improve the management of diabetes. **F7**

The authors thank C. A. Tse (School of Biological Sciences, University of Auckland, Auckland, New Zealand) for outstanding management, administrative assistance, and critical reading of the manuscript; A. Petzer, S. Johnson, Dr. J. Aitken, and C. C. H. Cheung for technical assistance; and the two anonymous reviewers for comprehensive analysis of the manuscript and for numerous insightful comments and suggestions that substantively strengthened the work. This work was funded by grants from Endocore Research Associates; the Maurice and Phyllis Paykel Trust; Lottery Health (New Zealand); the Auckland Medical Research Foundation; the University of Auckland; the Department of Education (New Zealand), through a grant to the Maurice Wilkins Centre of Excellence for Molecular BioDiscovery; by program grants from the Ministry for Business, Innovation, and Employment, New Zealand, and the Health Research Council of New Zealand. The study was facilitated by the Manchester Biomedical Research Centre and the UK National Institute for Health Research Greater Manchester Comprehensive Local Research Network.

## REFERENCES

- Cooper, G. J. S., Willis, A. C., Clark, A., Turner, R. C., Sim, R. B., and Reid, K. B. M. (1987) Purification and characterization of a peptide from amyloid-rich pancreases of type 2 diabetic patients. *Proc. Natl. Acad. Sci. U. S. A.* **84**, 8628–8632
- Westermarck, P., Wernstedt, C., Wilander, E., Hayden, D. W., O'Brien, T. D., and Johnson, K. H. (1987) Amyloid fibrils in human insulinoma and islets of Langerhans of the diabetic cat are derived from a neuropeptide-like protein also present in normal islet cells. *Proc. Natl. Acad. Sci. U. S. A.* **84**, 3881–3885
- Cooper, G. J. S. (1994) Amylin compared with calcitonin gene-related peptide: structure, biology, and relevance to metabolic disease. *Endocr. Rev.* **15**, 163–201
- Lukinius, A., Wilander, E., Westermarck, G. T., Engström, U., and Westermarck, P. (1989) Co-localization of islet amyloid polypeptide and insulin in the B cell secretory granules of the human pancreatic islets. *Diabetologia* **32**, 240–244
- Cooper, G. J. S., Day, A. J., Willis, A. C., Roberts, A. N., Reid, K. B. M., and Leighton, B. (1989) Amylin and the amylin gene: structure, function and relationship to islet amyloid and to diabetes mellitus. *Biochim. Biophys. Acta* **1014**, 247–258
- Westermarck, P., Engström, U., Johnson, K. H., Westermarck, G. T., and Betsholtz, C. (1990) Islet amyloid polypeptide: pinpointing amino acid residues linked to amyloid fibril formation. *Proc. Natl. Acad. Sci. U. S. A.* **87**, 5036–5040
- Green, J. D., Goldsbury, C., Kistler, J., Cooper, G. J. S., and Aebi, U. (2004) Human amylin oligomer growth and fibril elongation define two distinct phases in amyloid formation. *J. Biol. Chem.* **279**, 12206–12212
- Butler, A. E., Janson, J., Bonner-Weir, S., Ritzel, R., Rizza, R. A., and Butler, P. C. (2003) Beta cell deficit and increased beta-cell apoptosis in humans with type 2 diabetes. *Diabetes* **52**, 102–110
- Kahn, S. E., Andrikopoulos, S., and Verchere, C. B. (1999) Islet amyloid: a long-recognized but underappreciated pathological feature of type 2 diabetes. *Diabetes* **48**, 241–253
- Lorenzo, A., Razzaboni, B., Weir, G. C., and Yankner, B. A. (1994) Pancreatic islet cell toxicity of amylin associated with type-2 diabetes mellitus. *Nature* **368**, 756–760
- Goldsbury, C. S., Cooper, G. J. S., Goldie, K. N., Müller, S. A., Saafi, E. L., Gruijters, W. T. M., Misur, M. P., Engel, A., Aebi, U., and Kistler, J. (1997) Polymorphic fibrillar assembly of human amylin. *J. Struct. Biol.* **119**, 17–27
- Kapurniotu, A. (2001) Amyloidogenicity and cytotoxicity of islet amyloid polypeptide. *Biopolymers* **60**, 438–459
- Zhang, S., Liu, J. X., Saafi, E. L., and Cooper, G. J. S. (1999) Induction of apoptosis by human amylin in RINm5F islet beta-cells is associated with enhanced expression of p53 and p21(WAF1/CIP1). *FEBS Lett.* **455**, 315–320
- Cooper, G. J. S., Aitken, J. F., and Zhang, S. (2010) Is type 2 diabetes an amyloidosis and does it really matter (to patients)? *Diabetologia* **53**, 1011–1016
- Janson, J., Soeller, W. C., Roche, P. C., Nelson, R. T., Torchia, A. J., Kreutter, D. K., and Butler, P. C. (1996) Spontaneous diabetes mellitus in transgenic mice expressing human islet amyloid polypeptide. *Proc. Natl. Acad. Sci. U. S. A.* **93**, 7283–7288
- Zraika, S., Hull, R. L., Verchere, C. B., Clark, A., Potter, K. J., Fraser, P. E., Raleigh, D. P., and Kahn, S. E. (2010) Toxic oligomers and islet beta cell death: guilty by association or convicted by circumstantial evidence? *Diabetologia* **53**, 1046–1056
- Zhang, S., Liu, H., Yu, H., and Cooper, G. J. S. (2008) Fas-associated death receptor signaling evoked by human amylin in islet beta-cells. *Diabetes* **57**, 348–356
- Rumora, L., Hadzija, M., Barisic, K., Maysinger, D., and Grubiic, T. Z. (2002) Amylin-induced cytotoxicity is associated with activation of caspase-3 and MAP kinases. *Biol. Chem.* **383**, 1751–1758
- Zhang, S., Liu, H., Liu, J. X., Tse, C. A., Dragunow, M., and Cooper, G. J. S. (2006) Activation of activating transcription factor 2 by p38 MAP kinase during apoptosis induced by human amylin in cultured pancreatic beta-cells. *FEBS J.* **273**, 3779–3791
- Zhang, S., Liu, J. X., Dragunow, M., and Cooper, G. J. S. (2003) Fibrillogenic amylin evokes islet beta-cell apoptosis through linked activation of a caspase cascade and JNK1. *J. Biol. Chem.* **278**, 52810–52819
- Zhang, S., Liu, J. X., MacGibbon, G., Dragunow, M., and Cooper, G. J. S. (2002) Increased expression and activation of c-Jun contributes to human amylin-induced apoptosis in pancreatic islet beta-cells. *J. Mol. Biol.* **324**, 271–285
- Janson, J., Ashley, R. H., Harrison, D., McIntyre, S., and Butler, P. C. (1999) The mechanism of islet amyloid polypeptide toxicity is membrane disruption by intermediate-sized toxic amyloid particles. *Diabetes* **48**, 491–498
- Janciauskiene, S., and Ahren, B. (2000) Fibrillar islet amyloid polypeptide differentially affects oxidative mechanisms and lipoprotein uptake in correlation with cytotoxicity in two insulin-producing cell lines. *Biochem. Biophys. Res. Commun.* **267**, 619–625
- Lin, C. Y., Gurlo, T., Kaye, R., Butler, A. E., Haataja, L., Glabe, C. G., and Butler, P. C. (2007) Toxic human islet amyloid polypeptide (h-IAPP) oligomers are intracellular, and vaccination to induce anti-toxic oligomer antibodies does not prevent h-IAPP-induced beta-cell apoptosis in h-IAPP transgenic mice. *Diabetes* **56**, 1324–1332
- Oyadomari, S., Koizumi, A., Takeda, K., Gotoh, T., Akira, S., Araki, E., and Mori, M. (2002) Targeted disruption of the chop gene delays endoplasmic reticulum stress-mediated diabetes. *J. Clin. Invest.* **109**, 525–532
- Zraika, S., Hull, R. L., Udayasankar, J., Aston-Mourney, K., Subramanian, S. L., Kisilevsky, R., Szarek, W. A., and Kahn, S. E. (2009) Oxidative stress is induced by islet amyloid formation

- and time-dependently mediates amyloid-induced beta cell apoptosis. *Diabetologia* **52**, 626–635
27. Konarkowska, B., Aitken, J. F., Kistler, J., Zhang, S., and Cooper, G. J. S. (2006) The aggregation potential of human amylin determines its cytotoxicity towards islet beta-cells. *FEBS J.* **273**, 3614–3624
  28. Meier, J. J., Kaye, R., Lin, C. Y., Gurlo, T., Haataja, L., Jayasinghe, S., Langen, R., Glabe, C. G., and Butler, P. C. (2006) Inhibition of human IAPP fibril formation does not prevent beta-cell death: evidence for distinct actions of oligomers and fibrils of human IAPP. *Am. J. Physiol. Endocrinol. Metab.* **291**, E1317–E1324
  29. Ritzel, R. A., Meier, J. J., Lin, C. Y., Veldhuis, J. D., and Butler, P. C. (2007) Human islet amyloid polypeptide oligomers disrupt cell coupling, induce apoptosis, and impair insulin secretion in isolated human islets. *Diabetes* **56**, 65–71
  30. Hull, R. L., Westermark, G. T., Westermark, P., and Kahn, S. E. (2004) Islet amyloid: a critical entity in the pathogenesis of type 2 diabetes. *J. Clin. Endocrinol. Metab.* **89**, 3629–3643
  31. Maedler, K., and Donath, M. Y. (2004) Beta-cells in type 2 diabetes: a loss of function and mass. *Hormone Res.* **62**(Suppl. 3), 67–73
  32. Butler, A. E., Jang, J., Gurlo, T., Carty, M. D., Soeller, W. C., and Butler, P. C. (2004) Diabetes due to a progressive defect in beta-cell mass in rats transgenic for human islet amyloid polypeptide (HIP Rat): a new model for type 2 diabetes. *Diabetes* **53**, 1509–1516
  33. D'Alessio, D. A., Verchere, C. B., Kahn, S. E., Hoagland, V., Baskin, D. G., Palmiter, R. D., and Ensinck, J. W. (1994) Pancreatic expression and secretion of human islet amyloid polypeptide in a transgenic mouse. *Diabetes* **43**, 1457–1461
  34. Fox, N., Schrementi, J., Nishi, M., Ohagi, S., Chan, S. J., Heisserman, J. A., Westermark, G. T., Leckström, A., Westermark, P., and Steiner, D. F. (1993) Human islet amyloid polypeptide transgenic mice as a model of non-insulin-dependent diabetes mellitus (NIDDM). *FEBS Lett.* **323**, 40–44
  35. Höppener, J., Verbeek, J., de Koning, E., Oosterwijk, C., van Hulst, K., Visser-Vernooy, H., Hofhuis, F., van Gaalen, S., Berends, M., Hackeng, W., Jansz, H., Morris, J., Clark, A., Capel, P., and Lips, C. (1993) Chronic overproduction of islet amyloid polypeptide/amylin in transgenic mice: lysosomal localization of human islet amyloid polypeptide and lack of marked hyperglycaemia or hyperinsulinaemia. *Diabetologia* **36**, 1258–1265
  36. Butler, A. E., Janson, J., Soeller, W. C., and Butler, P. C. (2003) Increased beta-cell apoptosis prevents adaptive increase in beta-cell mass in mouse model of type 2 diabetes: evidence for role of islet amyloid formation rather than direct action of amyloid. *Diabetes* **52**, 2304–2314
  37. Verchere, C. B., D'Alessio, D. A., Palmiter, R. D., Weir, G. C., Bonner-Weir, S., Baskin, D. G., and Kahn, S. E. (1996) Islet amyloid formation associated with hyperglycemia in transgenic mice with pancreatic beta cell expression of human islet amyloid polypeptide. *Proc. Natl. Acad. Sci. U. S. A.* **93**, 3492–3496
  38. Wong, W. P., Scott, D. W., Chuang, C., Zhang, S., Liu, H., Ferreira, A., Saafi, E. L., Choong, Y.-S., and Cooper, G. J. S. (2008) Spontaneous diabetes in hemizygous human amylin transgenic mice that developed neither islet amyloid nor peripheral insulin resistance. *Diabetes* **57**, 2733–2744
  39. Aitken, J. F., Loomes, K. M., Scott, D. W., Reddy, S., Phillips, A. R. J., Pricic, G., Fernando, C., Zhang, S., Broadhurst, R., L'Huillier, P., and Cooper, G. J. S. (2010) Tetracycline treatment retards the onset and slows the progression of diabetes in human amylin/islet amyloid polypeptide transgenic mice. *Diabetes* **59**, 161–171
  40. Couce, M., Kane, L. A., O'Brien, T. D., Charlesworth, J., Soeller, W., McNeish, J., Kreutter, D., Roche, P., and Butler, P. C. (1996) Treatment with growth hormone and dexamethasone in mice transgenic for human islet amyloid polypeptide causes islet amyloidosis and beta-cell dysfunction. *Diabetes* **45**, 1094–1011
  41. American Diabetes Association (2013) Diagnosis and classification of diabetes mellitus. *Diabetes Care* **36**(Suppl. 1), S67–S74
  42. Bustin, S. A., Benes, V., Garson, J. A., Hellemans, J., Huggett, J., Kubista, M., Mueller, R., Nolan, T., Pfaffl, M. W., Shipley, G. L., Vandesompele, J., and Wittwer, C. T. (2009) The MIQE guidelines: minimum information for publication of quantitative real-time PCR experiments. *Clin. Chem.* **55**, 611–622
  43. Bonner-Weir, S. (2001) Beta-cell turnover: its assessment and implications. *Diabetes* **50**(Suppl. 1), S20–S24
  44. Kaye, R., Head, E., Thompson, L., McIntire, T., Milton, S., Cotman, C., and Glabe, C. (2003) Common structure of soluble amyloid oligomers implies common mechanism of pathogenesis. *Science* **300**, 486–489
  45. In't Veld, P. (2011) Insulinitis in human type 1 diabetes: the quest for an elusive lesion. *Islets* **3**, 131–138
  46. Hull, R. L., Andrikopoulos, S., Verchere, C. B., Vidal, J., Wang, F., Cnop, M., Prigeon, R. L., and Kahn, S. E. (2003) Increased dietary fat promotes islet amyloid formation and  $\beta$ -cell secretory dysfunction in a transgenic mouse model of islet amyloid. *Diabetes* **52**, 372–379
  47. Soeller, W. C., Janson, J., Hart, S. E., Parker, J. C., Carty, M. D., Stevenson, R. W., Kreutter, D. K., and Butler, P. C. (1998) Islet amyloid-associated diabetes in obese A<sup>Y</sup>/a mice expressing human islet amyloid polypeptide. *Diabetes* **47**, 743–750
  48. Kaye, R., and Glabe, C. G. (2006) Conformation-dependent anti-amyloid oligomer antibodies. *Methods Enzymol.* **413**, 326–344
  49. Zhao, H. L., Sui, Y., Guan, J., He, L., Gu, X. M., Wong, H. K., Baum, L., Lai, F. M. M., Tong, P. C. Y., and Chan, J. C. N. (2009) Amyloid oligomers in diabetic and nondiabetic human pancreas. *Transl. Res.* **153**, 24–32
  50. Westermark, G. T., Gebre-Medhin, S., Steiner, D. F., and Westermark, P. (2000) Islet amyloid development in a mouse strain lacking endogenous islet amyloid polypeptide (IAPP) but expressing human IAPP. *Mol. Med.* **6**, 998–1007
  51. Gong, W., Liu, Z. H., Zeng, C. H., Peng, A., Chen, H. P., Zhou, H., and Li, L. S. (2007) Amylin deposition in the kidney of patients with diabetic nephropathy. *Kidney Int.* **72**, 213–218
  52. Despa, S., Margulies, K. B., Chen, L., Knowlton, A. A., Havel, P. J., Taegtmeier, H., Bers, D. M., and Despa, F. (2012) Hyperamylinemia contributes to cardiac dysfunction in obesity and diabetes: a study in humans and rats. *Circ. Res.* **110**, 598–608

Received for publication April 23, 2014.  
Accepted for publication August 4, 2014.